# ORIGINAL ARTICLE

# Non-invasive evaluation of coronary heart disease in patients with chronic kidney disease using photoplethysmography

Turgay Saritas [1], Ruth Greber[1], Boudewijn Venema[2], Victor G. Puelles[1,3,4], Sabine Ernst[1], Vladimir Blazek[2], Jürgen Floege[1], Steffen Leonhardt[2] and Georg Schlieper [1,5]

[1]Nephrology and Clinical Immunology, University Hospital RWTH Aachen, Germany, [2]Helmholtz Institute for Biomedical Engineering, RWTH Aachen University, Aachen, Germany, [3]Department of Anatomy and Developmental Biology, Monash University, Melbourne, Victoria, Australia, [4]III. Department of Medicine, University Medical Center Hamburg-Eppendorf, Hamburg, Germany and [5]Center for Nephrology, Hypertension, and Metabolic Diseases, Hannover, Germany

Correspondence and offprint requests to: Turgay Saritas; E-mail: tsaritas@ukaachen.de

## ABSTRACT

**Background.** Chronic kidney disease (CKD) patients have an increased risk for coronary artery disease (CAD) and myocardial infarction. Therefore, there is a need to identify CKD patients at high risk of CAD. Coronary angiography, the gold standard for detecting CAD, carries a risk of serious adverse events.

**Methods.** Here, we assessed the validity of a novel non-invasive reflectance mode photoplethysmography (PPG) sensor for the evaluation of CAD in patients with advanced CKD. PPG signals were generated using green and infrared wavelengths and recorded from fingers of 98 patients. The detected signal has the shape of the pulse wave contour carrying information about the vascular system, that is, arterial stiffness. We studied four patient groups: (i) controls—patients without CKD or CAD; (ii) CKD alone; (iii) CAD alone (confirmed by coronary angiography); and (iv) CKD and CAD combined.

**Results.** With advancing age, we observed a steeper ascending signal during systole and greater signal decline during diastole (infrared wavelength: Slopes 4–6, $P = 0.002$, $P = 0.003$ and $P = 0.014$, respectively; green wavelength: Slopes 2–3, $P = 0.006$ and $P = 0.005$, respectively). Presence of CAD was associated with a slower signal decline during diastole in CKD patients compared with those without CAD (infrared wavelength: Slope 1, $P = 0.012$). CKD was associated with lower blood volume amplitude during each cardiac cycle compared with those without CKD (R-value, $P = 0.022$).

**Conclusions.** PPG signal analyses showed significant differences between our groups, and it may be a potentially useful tool for the detection of CAD in CKD patients.

**Keywords:** chronic kidney disease, coronary artery disease, photoplethysmography, vascular stiffness

## INTRODUCTION

Cardiovascular diseases (CVD) such as coronary artery disease (CAD) represent the main causes of morbidity and mortality in patients with chronic kidney disease (CKD) [1, 2]. There is significant interest in cardiac screening tests and their ability to identify CAD in CKD patients [3]. Although coronary angiography is the gold standard for detecting CAD, it is invasive, costly and carries the risk of nephrotoxicity (incidence of 3.3–16.5%), arrhythmia (incidence of 0.1–4.3%), peri-procedural myocardial infarction (defined by elevation of cardiac biomarkers; incidence of 5–30%), embolic events (incidence of 0.6–1.9%) and artery injury (incidence of 0.2–1%) [4–7].

Arterial stiffness secondary to arteriosclerosis and endothelial dysfunction has been recognized as an independent predictor of incident CAD and all-cause mortality in the general population and in patients with CKD [8, 9]. Arterial stiffness is characterized by a reduced capability of an artery to expand and contract in response to blood pressure changes [10]. It can be determined by digital volume pulse analysis with photoplethysmography (PPG) [11]. PPG, a low-cost non-invasive optical technique, is easy to setup and operator-independent—all great advantages for direct clinical application and reproducibility. The detected signal has the shape of the pulse wave contour and contains information about arterial stiffness [10]. By analysing the PPG signal, various vital signs [e.g. heart rate (HR), respiratory rate (RR), blood oxygenation, blood pressure and vasomotion] can be measured in parallel to diagnose and monitor diseases such as CVD, sleep apnoea or diabetes mellitus [12–15].

Light in the range red to near infrared is usually used for transmission mode PPG sensors since it better penetrates tissue than green light [16]. However, when reflectance mode PPG sensors are used, green light might also be suitable for estimation of arterial stiffness [17]. The aim of the study was to identify PPG signal parameters, which are significantly influenced by the presence of angiographically confirmed CAD in patients with CKD. For this purpose, we used a novel reflective PPG sensor to detect separately the reflection of green and infrared light and to analyse PPG signal.

## MATERIALS AND METHODS

### Study design

The study protocol was approved by the Local Clinical Research Ethics Committee and conforms to the principles outlined in the Declaration of Helsinki. Written informed consent of all patients was obtained. A total of 143 patients from the Cardio-Renal Inpatient Unit, University Hospital Aachen, Germany, were enrolled in the study (Figure 1). Data of six patients were excluded from all analyses due to contradictory statements made by patient or medical report about comorbidities. Data of one patient were excluded due to the withdrawal of the written informed consent. Data of another 10 patients were excluded due to technical problems (transfer of PPG signals to hardware). The remaining 126 patients were separated into four groups: (i) controls—patients without CKD or CAD ($n = 30$); (ii) CKD alone ($n = 28$); (iii) CAD alone ($n = 36$); and (iv) CKD and CAD combined ($n = 32$). CAD was defined as significant coronary stenosis ($\geq$70% stenosis) as detected by coronary angiography [18]. Patients were considered negative for CAD when significant stenosis was excluded during coronary angiography. A maximum of 1 year between coronary angiography and PPG measurements was accepted in the present study. Patients with normal kidney function had an estimated glomerular filtration rate (eGFR) >60 mL/min/1.73 m$^2$ and no albuminuria. All patients with CKD had an eGFR <30 mL/min/1.73 m$^2$ (CKD

Stages 4 and 5). We chose Stages 4 and 5 because of a higher rate of CV events in these sub-populations [19]. Diabetes mellitus was defined as having an HbA$_{1C}$ level of $\geq$6.5% and/or the intake of any anti-diabetic medication. Hypertension was given having either a systolic blood pressure of $\geq$140 mmHg and/or a diastolic blood pressure of $\geq$90 mmHg and/or receiving antihypertensive medication.

PPG signals were measured simultaneously on the left and right index finger. All patients rested for 10 min and PPG recordings were carried out for at least 120 s. During the measurements, patients were kept in a quiet environment, and breathed normally while resting in a supine position. PPG recordings in dialysis patients were performed on non-dialysis days. Indices derived from signals were averaged over 120 s. The PPG signal is composed of alternating (AC) and static (DC) components (Figure 2A). The AC pulsatile waveform is attributed to synchronous cardiac changes in blood volume with each heartbeat, while the DC is the static component of the signal, also containing slow frequencies due to respiration, sympathetic nervous system activity and thermoregulation. The quality of the detected raw PPG signals was evaluated by calculation of the signal-to-noise ratio (SNR):

$$\text{SNR} = 20\log\left(\frac{\sum_{0,\ 15\ HZ}^{3\ Hz} \text{PSD}\ (f)}{\sum_{30\ Hz}^{\infty} \text{PSD}\ (f)}\right) \text{dB}$$

The integral of AC component (0, 15–3 Hz) is defined as signal. Signal components of the power spectral density (PSD) higher than 30 Hz are defined as noise [20]. Only signal sequences of an SNR >12 dB for >5 s were used for statistical analyses. PPG signals of 98 patients of the remaining 126 patients fulfilled the SNR criteria and entered into the present analyses.

### Sensor system

The reflectance mode PPG sensor has been developed by the Philips Chair for Medical Information Technology (RWTH Aachen, Germany) in collaboration with the CiS Institute for Microsystems and Photovoltaics (Erfurt, Germany), and was first described in 2009 [21], and has been validated in several human trials [20, 22–25].

The PPG sensor contains two inversely connected light-emitting diodes (LED) with wavelengths of $\lambda1 = 525$ nm (green) and $\lambda2 = 948$ nm (infrared). The light emitted by these two LEDs is reflected by skin, tissue and blood (Figure 2B). The raw data generated by reflected light were pre-processed by the microcontroller (MSP430F1609, Texas Instruments, Inc.) and sent to the computer for visualization of PPG signal by using customized software ('LAVIMO-System'). Algorithms as described below were programed in MATLAB (The MathWorks Inc.) and were used for further automated signal processing [20, 24].

### Monitoring

**Heart rate.** The magnitude of the *Reflectance* PPG signal (*y*-value; termed as *Data*), which decreases during systole and increases during diastole over the time (*x*-value), depends on the blood volume in the capillary. HR was determined by calculation of all Data$_{max}$ per recorded time (Figure 2B).

**R-value.** The R-value takes the light intensity (*I*) of the reflected AC and the DC components of the green ($\lambda_{green}$) and infrared ($\lambda_{infrared}$) PPG signal into account [25, 26].

$$R = \frac{I_{AC}\ \lambda_{green}}{I_{DC}\ \lambda_{green}} \bigg/ \frac{I_{AC}\ \lambda_{infrared}}{I_{DC}\ \lambda_{infrared}}$$
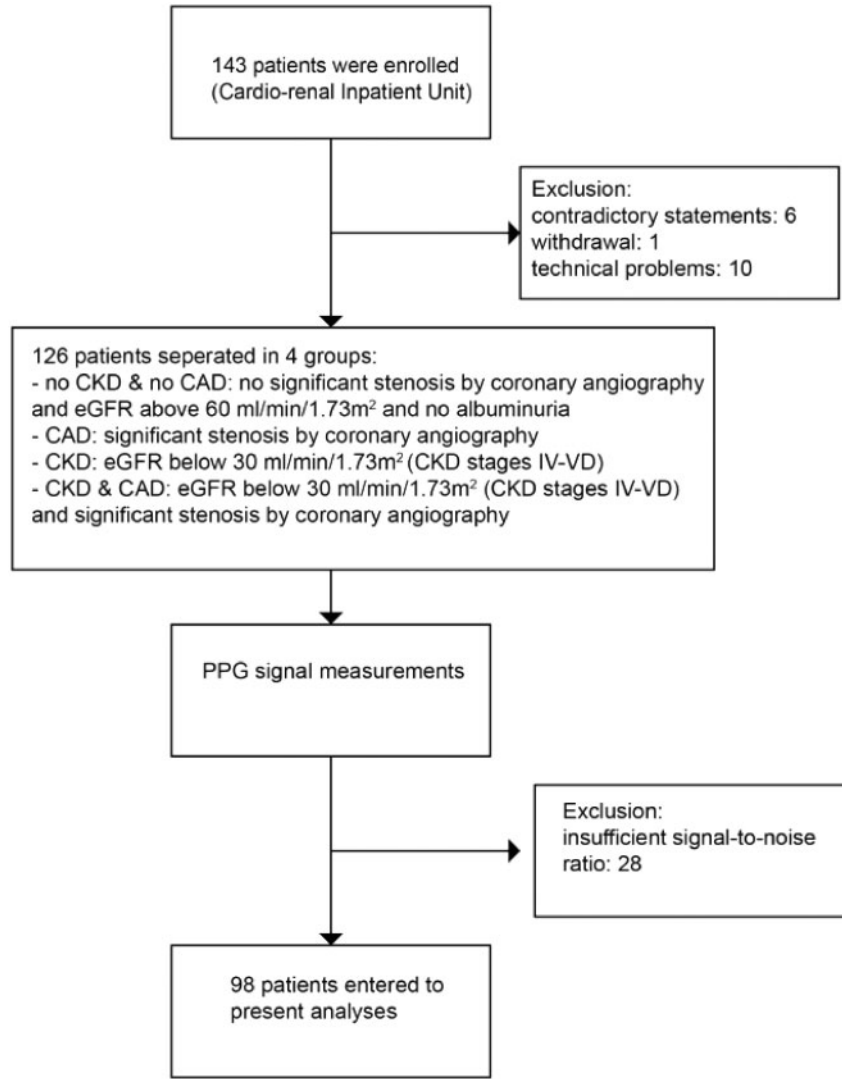
**FIGURE 1:** Flow chart of patients who met inclusion/exclusion criteria for the study population.
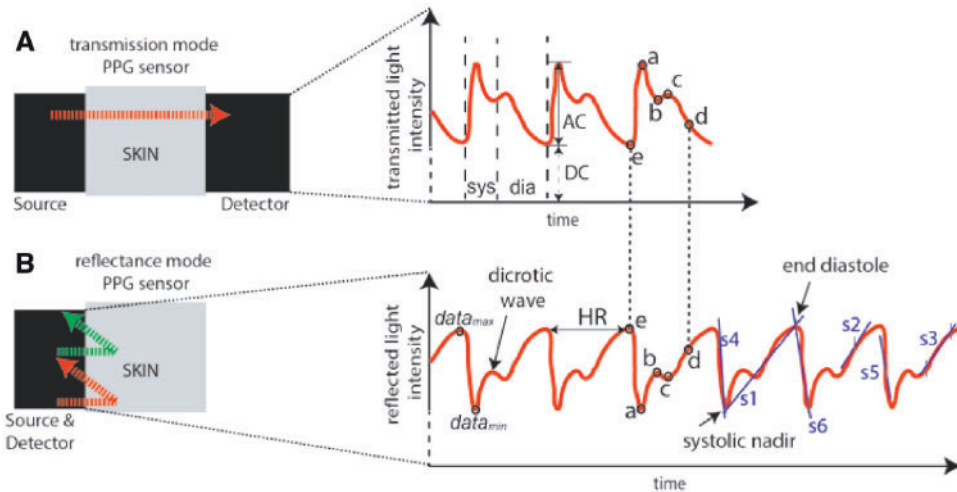


**FIGURE 2:** PPG sensor. (**A** and **B**) Comparison of transmission and reflectance mode PPG sensors. The signal intensity and shape of transmitted PPG signal (A) behaves inverse to PPG signal detected by a reflectance mode PPG sensor (B). sys, systole; dia, diastole; s1–s6, slope of the connecting lines 1–6.

with $AC = Data_{max} - Data_{min}$
and $DC = \frac{1}{2} \times (Data_{max} + Data_{min})$

**Respiratory rate.** The RR can be determined by the separation of amplitude fluctuations in PPG signal [25]. We chose a fifth-order Butterworth filter with cut-off frequencies 0.34 Hz and calculated all $Data_{min}$ per recorded time.

**PPG segments/slopes, dicrotic wave.** The systolic amplitude is an indicator of the pulsatile changes in blood volume, caused by arterial blood volume, which is directly proportional to local vascular distensibility. The dicrotic wave (b in Figure 2B) corresponds with the closing of aortic valve and separates systole from diastole [27]. We chose a fourth-order Butterworth filter with cut-off frequencies 3 Hz to calculate dicrotic wave. The wave is followed by a short dip of the PPG signal (c in Figure 2B), which is the result of the short increase in local blood pressure caused by the elastic recoil of the valves and aorta.

To analyse the effect of CAD on PPG signal in more detail, we divided the PPG curve in sections and measured the slope of each section (Figure 2B). We assume that all slopes are steeper when finger arterioles are stiffened (arterial stiffness causes both a greater signal peak during systole and a larger decline during diastole [10]).

Slope 1 (s1) is determined by the slope of the connecting line between minimum and maximum of reflected signal intensity. It correlates with the relative shift of blood volume during late systole and diastole.

$$\text{Slope } 1 = \frac{AC}{x_{max} - x_{min}} \times 200 \text{ (per seconds)}$$

S2 and s3 are characterized by changes of reflected light intensity after closure of the aortic valve during diastole. S2 is determined by the slope around the centre of the ascending curve (centre$_{asc}$) (Figure 2B). The centre of the ascending curve was determined by following formula:

$$\text{Centre}_{asc} = \frac{AC}{2} + \text{data} \ (x_{min})$$

$$\text{Slope } 2 = \frac{Data(x_{centre_{asc}} + 5) - Data(x_{centre_{asc}} - 5)}{11} \times 200 \text{ (per seconds)}$$

S3 is determined by the slope of the ascending part between one-third and two-thirds of the line between a and e (Figure 2B):

$$\text{Slope } 3 = \frac{Data(x_{centre_{asc}} + 15) - Data(x_{centre_{asc}} - 15)}{31} \times 200 \text{ (per seconds)}$$

S4, 5 and 6 describe the reflected light intensity during early systole. S4 is determined by the slope of the connecting line between e and a (Figure 2B):

$$\text{Slope } 4 = \frac{-AC}{x_{min} - x_{max}} \times 200 \text{ (per seconds)}$$

S5 is determined by the slope around the centre of the descending curve (centre$_{desc}$) (Figure 2B):

$$\text{Slope } 5 = \frac{Data(x_{centre_{desc}} + 5) - Data(x_{centre_{desc}} - 5)}{11} \times 200 \text{ (per seconds)}$$

S6 is determined by the slope of the descending part between one-third and two-thirds of the line between e and a (Figure 2B):

$$\text{Slope } 6 = \frac{Data(x_{centre_{desc}} + 15) - Data(x_{centre_{desc}} - 15)}{31} \times 200 \text{ (per seconds)}$$

The slope of those lines was normalized for HR and AC.

## Statistical analysis

The data were obtained and analysed by a single observer who was blinded in terms of the presence of CAD or CKD. Descriptive statistics were used to compare baseline clinical and demographic characteristics. The variables were tested for normality using graphic methods (histograms and quantile-quantile plot instead of Q–Q plot) and the Shapiro–Wilk test. Multifactorial repeated measures analysis of variance (ANOVA)/analysis of covariance (ANCOVA) were performed by accounting age, gender, site of measurement (left or right finger) and presence of diabetes mellitus as potential confounding factor. *Post hoc* analyses of parameters were performed when confounder-adjusted parameters differed between the groups. Paired *t*-test was performed to analyse differences between the arm with and without an arteriovenous (AV) fistula. P < 0.05 were considered significant. All statistical analyses were performed using SAS, version 9.4, and GraphPad Prism 6.01.

## RESULTS

### Demographic characteristics and comorbidity and influence of age on PPG signal parameters

Baseline clinical and demographic characteristics of the 98 patients entering the analyses are shown in Table 1. The mean age was significantly higher in patients with CKD and CAD compared with the group of patients with CKD (P = 0.049).

In all patients, age significantly and independently affected distinct sections of the PPG signal. In particular, using infrared wavelength, we observed advancing age with an augmented increase of PPG signal during systole (Table 2; s4–s6; P = 0.002, P = 0.003 and P = 0.014, respectively). By using the green wavelength, we detected an increase of age with a greater decline of PPG signal during diastole (Table 2; s2 and s3; P = 0.006 and P = 0.005, respectively).

### Influence of CAD on PPG signal parameters

To determine whether the presence of CAD in CKD patients affects PPG signal parameters, PPG data were corrected for age, sex and diabetes mellitus. No differences in PPG signal parameters were detectable between the left and right index finger (data not shown). By using the infrared wavelength, the presence of CAD in patients with CKD was associated with a slower decline of signal during diastole (Table 3; Figure 3A; s1; P = 0.012). The PPG signal obtained by the green wavelength was not different between the groups (Table 4).

### Influence of CKD and AV fistula on PPG signal parameters

Although the primary aim of the study was to evaluate CAD in CKD patients, we also asked whether CKD or the presence of an AV fistula alters the shape of the PPG signal. We observed that

**Table 1.** Basic characteristics of the participants who fulfilled the SNR requirements

| Characteristic | All ($n = 98$) | No CKD and no CAD ($n = 27$) | CAD ($n = 31$) | CAD and CKD ($n = 21$) | CKD ($n = 19$) |
|---|---|---|---|---|---|
| Age, mean ± SD, years | 67.0 ± 13.4 | 62.3 ± 17.0 | 69.0 ± 11.3 | 72.3 ± 12.0 | 64.2 ± 13.3 |
| BMI, mean ± SD, kg/m$^2$ | 26.5 ± 6.5 | 25.9 ± 7.9 | 27.4 ± 4.3 | 25.6 ± 4.8 | 27.6 ± 7.9 |
| Male, % | 65 | 52 | 94 | 52 | 53 |
| eGFR, mean ± SD, mL/min/1.73 m$^2$ | N/A | >60 | >60 | 17 ± 11 | 17 ± 9 |
| Systolic blood pressure, mean ± SD, mmHg | 131 ± 21 | 127 ± 14 | 130 ± 16 | 135 ± 25 | 134 ± 31 |
| Diastolic blood pressure, mean ± SD, mmHg | 76 ± 14 | 76 ± 14 | 74 ± 10 | 74 ± 12 | 78 ± 15 |
| Hypertension, % | 75 | 48 | 81 | 91 | 84 |
| Diabetes mellitus, % | 26 | 11 | 16 | 52 | 32 |
| Aortic stenosis, % | 17 | 22 | 10 | 24 | 16 |
| Chronic heart failure, % | 48 | 52 | 52 | 33 | 53 |
| AV fistula, % | 9 | 0 | 0 | 24 | 21 |

BMI, body mass index; N/A, not applicable.

**Table 2.** Association between age and PPG signal

| Parameter | P-value | |
|---|---|---|
| | $\lambda$ green | $\lambda$ infrared |
| HR | 0.84 | 0.80 |
| RR | 0.94 | 0.35 |
| AC | 0.11 | 0.08 |
| DC | 0.43 | 0.54 |
| R-value | 0.27 | 0.28 |
| Dicrotic wave | 0.71 | 0.22 |
| Slope 1/(AC×HR) | 0.49 | 0.24 |
| Slope 2/(AC×HR) | 0.006* | 0.36 |
| Slope 3/(AC×HR) | 0.005* | 0.27 |
| Slope 4/(AC×HR) | 0.13 | 0.002* |
| Slope 5/(AC×HR) | 0.15 | 0.003* |
| Slope 6/(AC×HR) | 0.23 | 0.014* |

*$P < 0.05$ were considered significant.

the R-values, which correlate with the blood volume amplitude during systole, were significantly lower in CKD patients compared with patients with normal kidney function (Tables 3 and 4). This was true for the comparison of CKD patients with both control or CAD patients ($P = 0.021$ and $P = 0.036$, respectively) (Figure 3B).

Using the green wavelength, PPG signals were not different between the arm with an AV fistula versus those without (Table 5). The infrared wavelength-derived PPG signal showed significantly steeper increase in blood volume during systole in the arm with AV fistula compared with the arm without AV fistula (Table 5; s2 and s3; $P = 0.041$ and $P = 0.048$, respectively).

### Signal quality

We observed that our programme counted fewer PPG-derived values for HR, RR and R-value for each patient, when they were generated by green light as compared with infrared light (Supplementary data, Table S1). In contrast, fewer values for s1–s6 were counted when infrared light was used (Supplementary data, Table S1).

### DISCUSSION

In this work, we evaluated the potential of a novel reflectance PPG sensor as a non-invasive tool to identify PPG signal parameters, which are significantly influenced by the presence of angiographically confirmed CAD in patients with CKD.

Infrared wavelength is usually used to generate PPG signals, but green-wavelength PPG sensors are becoming increasingly popular for their higher specificity for detecting vascular alterations compared with infrared light [28]. The current study compared the performance of infrared and green wavelength and found significant alterations in PPG signal with advancing age and presence of CAD. Our findings suggest that the blood volume decreases more slowly during diastole in capillaries of CKD patients with CAD compared with CKD patients without CAD, and we speculate that this is explained by changes in arterial stiffness and/or changes in the tone of small vessels. However, this observation was limited to PPG signals generated by infrared LED. Sollinger *et al.* [29] demonstrated in a small subgroup analysis that patients with CKD had a greater PPG-derived stiffness index when they had a history of CAD compared with CKD patients without CAD. Although the presence of subclinical CAD in CKD patients was not angiographically evaluated and the sample group was only around a dozen, this study supports our findings. Previous reports also demonstrated an independent relationship between arterial stiffness and age [29–31]. In agreement with these reports, we observed in all patients that PPG slopes were significantly influenced by age.

We found that the presence of CKD was associated with lower blood volume amplitudes, as estimated by measuring the R-value. Especially, the lower AC values in CKD patients caused these differences. AC (blood volume amplitude in the finger capillaries during each cardiac cycle) is low in case of decreased blood volume shifts/pulsations, decreased venous blood volume or due to peripheral vasoconstriction [32]. Further studies are needed to clarify the reason for lower AC values in CKD patients. For example, a role of renin–angiotensin–aldosterone system herein is possible. So far, there is evidence that angiotensin II and aldosterone, both hormones that are linked to CKD, contribute significantly to arterial stiffness [33].

We tested whether the presence of a dialysis AV fistula influences the shape of the PPG signal. Using the infrared wavelength, we detected significantly steeper increase in blood volume during systole in the arm with an AV fistula compared with the arm without AV fistula, suggesting an increased small vascular tone in the shunt arm. AV fistula undergoes vascular remodelling and causes an altered haemodynamic situation and endothelial dysfunction in the dialysis arm [34]. Endothelial dysfunction is associated with reduced endothelial vasodilator

**Table 3.** Analysis of PPG signals (infrared wavelength)

| Parameter | No CKD/no CAD | CAD | CAD/CKD | CKD |
|---|---|---|---|---|
| HR (beats per minute) | 70 ± 10 | 68 ± 9 | 67 ± 9 | 72 ± 11 |
| RR (breaths per minute) | 15 ± 1 | 14 ± 1 | 15 ± 1 | 15 ± 1 |
| AC | 18 342 ± 12 909 | 24 731 ± 15 425 | 18 904 ± 14 477 | 16 106 ± 15 348 |
| DC | 1 298 369 ± 400 326 | 1 330 661 ± 411 236 | 1 355 604 ± 340 176 | 1 269 757 ± 356 132 |
| R-value | 0.32 ± 0.29* | 0.30 ± 0.13* | 0.21 ± 0.11* | 0.21 ± 0.11* |
| Dicrotic wave | 2116 ± 1564 | 2732 ± 1872 | 2116 ± 1442 | 1505 ± 1024 |
| Slope 1/(AC×HR) (per second) | 0.025 ± 0.004* | 0.025 ± 0.003* | 0.025 ± 0.003* | 0.027 ± 0.003* |
| Slope 2/(AC×HR) (per second) | 0.026 ± 0.008 | 0.028 ± 0.012 | 0.031 ± 0.015 | 0.029 ± 0.01 |
| Slope 3/(AC×HR) (per second) | 0.028 ± 0.08 | 0.029 ± 0.11 | 0.033 ± 0.015 | 0.032 ± 0.01 |
| Slope 4/(AC×HR) (per second) | −0.047 ± 0.006 | −0.0477 ± 0.0073 | −0.049 ± 0.008 | −0.045 ± 0.006 |
| Slope 5/(AC×HR) (per second) | −0.07 ± 0.009 | −0.072 ± 0.01 | −0.07 ± 0.01 | −0.069 ± 0.007 |
| Slope 6/(AC×HR) (per second) | −0.67 ± 0.008 | −0.0684 ± 0.009 | −0.07 ± 0.011 | −0.066 ± 0.008 |

PPG signal-derived values were obtained from each group using the infrared wavelength. Values are presented as mean ± SD. Slope of the connecting lines 1–6 were adjusted for HR and AC. Between-group comparisons were made by two-way repeated measures ANOVA.
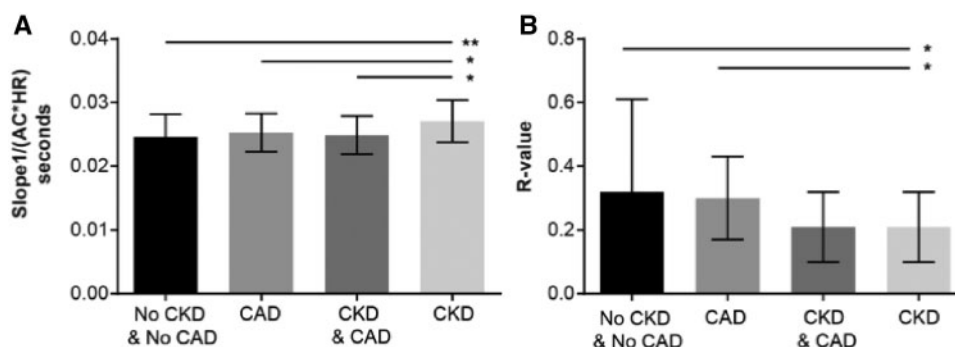*$P < 0.05$ were considered significant.



**FIGURE 3:** PPG signal-derived values for s1/(AC*HR) and R-value using infrared wavelength. Values for s1/(AC*HR) (**A**) and R-value (**B**) are presented as mean ± SD. Between-group comparisons were made by two-way repeated measures ANOVA and *post hoc* analysis. From each patient, $n = 118$–124 or $n = 87$–103 data points were recorded to quantify s1/(AC*HR) or R-value, respectively. $P < 0.05$ or 0.01 were considered significant (*) or highly significant (**). See also Table 3.

**Table 4.** Analysis of PPG signals (green wavelength)

| Parameter | No CKD and No CAD | CAD | CAD and CKD | CKD |
|---|---|---|---|---|
| HR (beats per minute) | 71 ± 10 | 67 ± 9 | 67 ± 9 | 72 ± 11 |
| RR (breaths per minute) | 14 ± 2 | 14 ± 1 | 14 ± 1 | 15 ± 1 |
| AC | 6826 ± 5937 | 7542 ± 7556 | 7535 ± 6355 | 6479 ± 8864 |
| DC | 116 766 ± 64 382 | 97 294 ± 63 317 | 101 091 ± 52 948 | 79 569 ± 45 502 |
| R-value | 0.32 ± 0.29* | 0.30 ± 0.13* | 0.21 ± 0.11* | 0.21 ± 0.11* |
| Dicrotic wave | 851 ± 752 | 793 ± 882 | 878 ± 852 | 509 ± 814 |
| Slope 1/(AC×HR) (per second) | 0.022 ± 0.004 | 0.023 ± 0.003 | 0.023 ± 0.003 | 0.032 ± 0.04 |
| Slope 2/(AC×HR) (per second) | 0.022 ± 0.007 | 0.022 ± 0.006 | 0.026 ± 0.01 | 0.022 ± 0.006 |
| Slope 3/(AC×HR) (per second) | 0.024 ± 0.007 | 0.024 ± 0.006 | 0.027 ± 0.009 | 0.024 ± 0.006 |
| Slope 4/(AC×HR) (per second) | −0.044 ± 0.010 | −0.047 ± 0.009 | −0.046 ± 0.008 | −0.044 ± 0.007 |
| Slope 5/(AC×HR) (per second) | −0.067 ± 0.015 | −0.071 ± 0.013 | −0.069 ± 0.012 | −0.067 ± 0.013 |
| Slope 6/(AC×HR) (per second) | −0.067 ± 0.014 | −0.067 ± 0.012 | −0.066 ± 0.011 | −0.06 ± 0.013 |

PPG signal-derived values were obtained from each group using the green wavelength. Values are presented as mean ± SD. Slope of the connecting lines 1–6 were adjusted for HR and AC. Between-group comparisons were made by two-way repeated measures ANOVA.
*P-values <0.05 were considered significant.

activity (mediated by nitric oxide, prostacyclin and bradykinin) and increased synthesis of vasoconstrictors (endothelin, angiotensin II and free oxygen radicals) [35, 36], resulting in an increased small vascular tone.

Our study has some limitations. The sample size was small, which limits our ability to detect a cut-off value for a blinded detection of CAD. However, we minimized the sample size effect by adjusting the parameters for age, sex and presence of diabetes mellitus. Despite PPG's wide range of applications, there are technical limitations. The PPG sensor can only detect dynamic changes of the blood volume at one spot per probe, thus PPG signal interpretation has to be discussed with

Table 5. PPG signal parameters recorded from the arm with AV fistula and arm without AV fistula

| Parameter | Green wavelength | | Infrared wavelength | |
|---|---|---|---|---|
| | AV fistula | No AV fistula | AV fistula | No AV fistula |
| HR (beats per minute) | 71 | 70 | 70 | 70 |
| RR (breaths per minute) | 15 | 15 | 16 | 15 |
| AC | 4262 | 5242 | 14 148 | 20 339 |
| DC | 74 327 | 83 279 | 1 192 405 | 1 326 814 |
| R-value | 0.22 | 0.22 | 0.22 | 0.22 |
| Dicrotic wave | 568 | 743 | 2020 | 1949 |
| Slope 1/(AC×HR) (per second) | 0.023 | 0.23 | 0.027 | 0.025 |
| Slope 2/(AC×HR) (per second) | 0.028 | 0.029 | 0.039* | 0.032* |
| Slope 3/(AC×HR) (per second) | 0.029 | 0.030 | 0.040* | 0.034* |
| Slope 4/(AC×HR) (per second) | −0.043 | −0.048 | −0.046 | −0.049 |
| Slope 5/(AC×HR) (per second) | −0.065 | −0.071 | −0.071 | −0.073 |
| Slope 6/(AC×HR) (per second) | −0.062 | −0.067 | −0.067 | −0.069 |

Mean PPG signal-derived values were obtained from each group using the green and infrared wavelength. Slope of the connecting lines 1–6 were adjusted for HR and AC. Asterisks marks values that were significantly different between arm with fistula and arm without fistula. $P < 0.05$ were considered as significant.

caution. A remote imaging PPG technology may overcome this limitation by detecting signal simultaneously from multiple sites [37]. Another technical limitation is that PPG is susceptible to signal artefacts. Therefore, we evaluated the quality of the detected PPG signal by calculation of the signal-to-noise ratio and had to exclude 22% of all enrolled patients. While PPG may detect CAD-associated changes in the vessels of investigation, we are aware that there are other factors that influence cardiac morbidity and mortality that we were unable to evaluate with PPG [38]. Patients with CAD and CKD have complex and severe microcirculatory alterations (i.e. abnormal coronary ischaemic events in the absence of significant stenosis) [39, 40], and randomized controlled trails are needed to assess the predictive capacity of PPG in determining CAD in patients with CKD.

In summary, PPG is an interesting technology due to its simplicity, low-cost and non-invasiveness, and PPG signal was affected by the presence of angiographically confirmed CAD in patients with advanced CKD. Although the use of PPG in CKD patients may represent a promising diagnostic tool and could help physicians to choose appropriate treatment, it requires further validation in larger prospective clinical cohorts.

## SUPPLEMENTARY DATA

Supplementary data are available at ckj online.

## ACKNOWLEDGEMENTS

## FUNDING

## CONFLICT OF INTEREST STATEMENT

None declared.

## REFERENCES

1. Heywood JT, Fonarow GC, Costanzo MR *et al*. High prevalence of renal dysfunction and its impact on outcome in 118, 465 patients hospitalized with acute decompensated heart failure: a report from the ADHERE database. *J Card Fail* 2007; 13: 422–430
2. Sowers JR. Diabetes mellitus and vascular disease. *Hypertension* 2013; 61: 943–947
3. Wang LW, Fahim MA, Hayen A *et al*. Cardiac testing for coronary artery disease in potential kidney transplant recipients: a systematic review of test accuracy studies. *Am J Kidney Dis* 2011; 57: 476–487
4. Tavakol M, Ashraf S, Brener SJ. Risks and complications of coronary angiography: a comprehensive review. *Glob J Health Sci* 2012; 4: 65–93
5. Ioannidis JP, Karvouni E, Katritsis DG. Mortality risk conferred by small elevations of creatine kinase-MB isoenzyme after percutaneous coronary intervention. *J Am Coll Cardiol* 2003; 42: 1406–1411
6. Bashore TM, Gehrig T. Cholesterol emboli after invasive cardiac procedures. *J Am Coll Cardiol* 2003; 42: 217–218
7. Applegate RJ, Sacrinty MT, Kutcher MA *et al*. Trends in vascular complications after diagnostic cardiac catheterization and percutaneous coronary intervention via the femoral artery, 1998 to 2007. *JACC Cardiovasc Interv* 2008; 1: 317–326
8. Vlachopoulos C, Aznaouridis K, Stefanadis C. Prediction of cardiovascular events and all-cause mortality with arterial stiffness: a systematic review and meta-analysis. *J Am Coll Cardiol* 2010; 55: 1318–1327
9. Mitchell GF, Hwang SJ, Vasan RS *et al*. Arterial stiffness and cardiovascular events: the Framingham Heart Study. *Circulation* 2010; 121: 505–511
10. Allen J. Photoplethysmography and its application in clinical physiological measurement. *Physiol Meas* 2007; 28: R1–R39
11. Millasseau SC, Kelly RP, Ritter JM *et al*. Determination of age-related increases in large artery stiffness by digital pulse contour analysis. *Clin Sci (Lond)* 2002; 103: 371–377
12. Karmakar C, Khandoker A, Penzel T *et al*. Detection of respiratory arousals using photoplethysmography (PPG) signal in

sleep apnea patients. *IEEE J Biomed Health Inform* 2014; 18: 1065–1073.

13. Karimipour H, Shandiz HT, Zahedi E. Diabetic diagnose test based on PPG signal and identification system. *J Biomed Sci Eng* 2009; 2: 465

14. Schafer A, Vagedes J. How accurate is pulse rate variability as an estimate of heart rate variability? A review on studies comparing photoplethysmographic technology with an electrocardiogram. *Int J Cardiol* 2013; 166: 15–29

15. Middleton PM, Chan GS, Marr S *et al.* Identification of high-risk acute coronary syndromes by spectral analysis of ear photoplethysmographic waveform variability. *Physiol Meas* 2011; 32: 1181–1192

16. Li K, Warren S. A wireless reflectance pulse oximeter with digital baseline control for unfiltered photoplethysmograms. *IEEE Trans Biomed Circuits Syst* 2012; 6: 269–278

17. Zakharov P, Talary MS, Caduff A. A wearable diffuse reflectance sensor for continuous monitoring of cutaneous blood content. *Phys Med Biol* 2009; 54: 5301

18. Patel MR, Calhoon JH, Dehmer GJ *et al.* ACC/AATS/AHA/ASE/ASNC/SCAI/SCCT/STS 2017 Appropriate Use Criteria for Coronary Revascularization in Patients With Stable Ischemic Heart Disease. A Report of the American College of Cardiology Appropriate Use Criteria Task Force, American Association for Thoracic Surgery, American Heart Association, American Society of Echocardiography, American Society of Nuclear Cardiology, Society for Cardiovascular Angiography and Interventions, Society of Cardiovascular Computed Tomography, and Society of Thoracic Surgeons. *J Am Coll Cardiol* 2017; 69(17): 2212–41

19. Schiffrin EL, Lipman ML, Mann JF. Chronic kidney disease: effects on the cardiovascular system. *Circulation* 2007; 116: 85–97

20. Venema B, Blanik N, Blazek V *et al.* Advances in reflective oxygen saturation monitoring with a novel in-ear sensor system: results of a human hypoxia study. *IEEE Trans Biomed Eng* 2012; 59: 2003–2010

21. Vogel S, Hulsbusch M, Hennig T *et al.* In-ear vital signs monitoring using a novel microoptic reflective sensor. *IEEE Trans Inf Technol Biomed* 2009; 13: 882–889

22. Vogel S, Hulsbusch M, Starke D *et al.* A system for assessing motion artifacts in the signal of a micro-optic in-ear vital signs sensor. *Conf Proc IEEE Eng Med Biol Soc* 2008; 2008: 510–513

23. Brodersen O, Römhild D, Starke D *et al.* In-ear acquisition of vital signs discloses new chances for preventive continuous cardiovascular monitoring. In: Leonhardt S, Falck T, Mähönen P (eds). *4th International Workshop on Wearable and Implantable Body Sensor Networks (BSN 2007): March 26–28, 2007 RWTH Aachen University*, Germany. Berlin, Heidelberg: Springer Berlin Heidelberg, 2007, 189–194

24. Vogel S, Hulsbusch M, Starke D *et al.* In-ear heart rate monitoring using a micro-optic reflective sensor. *Conf Proc IEEE Eng Med Biol Soc* 2007; 2007: 1375–1378

25. Venema B, Blanik N, Blazek V *et al.* A feasibility study evaluating innovative in-ear pulse oximetry for unobtrusive cardiovascular homecare monitoring during sleep. *IEEE EMBS Special Topic Conference on Point-of-Care (POC) Healthcare Technologies: synergy towards better global healthcare* 16–18 January 2013, Sheraton Bangalore at Brigade Gateway/ Institute of Electrical and Electronics Engineers. IEEE Engineering in Medicine and Biology Society, 124–127. More information: https://ieeexplore.ieee.org/document/6461300

26. Nitzan M, Romem A, Koppel R. Pulse oximetry: fundamentals and technology update. *Med Devices (Auckl)* 2014; 7: 231–239

27. Nara S, Kaur M, Verma KL. Novel notch detection algorithm for detection of dicrotic notch in PPG signals. *Int J Comp Appl* 2014; 86: 36–39.

28. Sun Y, Thakor N. Photoplethysmography revisited: from contact to noncontact, from point to imaging. *IEEE Trans Biomed Eng* 2016; 63: 463–477

29. Sollinger D, Mohaupt MG, Wilhelm A *et al.* Arterial stiffness assessed by digital volume pulse correlates with comorbidity in patients with ESRD. *Am J Kidney Dis* 2006; 48: 456–463

30. Guerin AP, Blacher J, Pannier B *et al.* Impact of aortic stiffness attenuation on survival of patients in end-stage renal failure. *Circulation* 2001; 103: 987–992

31. Blacher J, Safar ME, Guerin AP *et al.* Aortic pulse wave velocity index and mortality in end-stage renal disease. *Kidney Int* 2003; 63: 1852–1860

32. Korhonen I, Yli-Hankala A. Photoplethysmography and nociception. *Acta Anaesthesiol Scand* 2009; 53: 975–985

33. Aroor AR, McKarns S, Demarco VG *et al.* Maladaptive immune and inflammatory pathways lead to cardiovascular insulin resistance. *Metabolism* 2013; 62: 1543–1552

34. Remuzzi A, Bozzetto M. Biological and physical factors involved in the maturation of arteriovenous fistula for hemodialysis. *Cardiovasc Eng Technol* 2017; 8: 273–279

35. Zou Y, Dietrich H, Hu Y *et al.* Mouse model of venous bypass graft arteriosclerosis. *Am J Pathol* 1998; 153: 1301–1310

36. Kokubo T, Uchida H, Choi ET. Integrin alpha(v)beta(3) as a target in the prevention of neointimal hyperplasia. *J Vasc Surg* 2007; 45 (Suppl A): A33–A38

37. Sun Y, Papin C, Azorin-Peris V *et al.* Use of ambient light in remote photoplethysmographic systems: comparison between a high-performance camera and a low-cost webcam. *J Biomed Opt* 2012; 17: 037005

38. Yao Q, Pecoits-Filho R, Lindholm B *et al.* Traditional and non-traditional risk factors as contributors to atherosclerotic cardiovascular disease in end-stage renal disease. *Scand J Urol Nephrol* 2004; 38: 405–416

39. Niizuma S, Takiuchi S, Okada S *et al.* Decreased coronary flow reserve in haemodialysis patients. *Nephrol Dial Transplant* 2008; 23: 2324–2328

40. Sezer M, Ozcan M, Okcular I *et al.* A potential evidence to explain the reason behind the devastating prognosis of coronary artery disease in uraemic patients: renal insufficiency is associated with poor coronary collateral vessel development. *Int J Cardiol* 2007; 115: 366–372